European Journal of Pharmaceutical Sciences 189 (2023) 106559

Contents lists available at ScienceDirect

European Journal of Pharmaceutical Sciences

journal homepage: www.elsevier.com/locate/ejps

Interpreting permeability as a function of free drug fraction: The case studies of cyclodextrins and liposomes

Martina M. Tzanova [a], Lisa Nguyen [a], Federica Moretti [b], Mario Grassi [b], Greta Camilla Magnano [c], Dario Voinovich [c], Paul C. Stein [d], Marianne Hiorth [a], Massimiliano Pio di Cagno [a,*]

[a] Department of Pharmacy, Faculty of Mathematics and Natural Sciences, University of Oslo, Sem Saelands vei 3, 0371 Oslo, Norway
[b] Department of Engineering and Architecture, University of Trieste, Via Alfonso Valerio, 6/1, 34127 Trieste, Italy
[c] Department of Chemical and Pharmaceutical Sciences, University of Trieste, Via Alfonso Valerio, 6/1, 34127 Trieste, Italy
[d] Department of Physics, Chemistry and Pharmacy, University of Southern Denmark, 5230 Odense, Denmark

ARTICLE INFO

Keywords:
Free drug fraction
Absolute permeability coefficient
Inclusion complex
Drug diffusivity
Solubilization
PermeaPad®

ABSTRACT

In order to solubilize poorly soluble active pharmaceutical ingredients, various strategies have been implemented over the years, including the use of nanocarriers, such as cyclodextrins and liposomes. However, improving a drug's apparent solubility does not always translate to enhanced bioavailability. This work aimed to investigate to which extent complexation with cyclodextrins and incorporation into liposomes influence drug *in vitro* permeability and to find a mechanistic description of the permeation process. For this purpose, we investigated hydroxypropyl-β-cyclodextrin (HP-β-CD) and phosphatidylcholine liposomes formulations of three chemically diverse compounds (atenolol, ketoprofen and hydrocortisone). We studied drug diffusion of the formulations by UV-localized spectroscopy and advanced data fitting to extract parameters such as diffusivity and bound-/free drug fractions. We then correlated this information with *in vitro* drug permeability obtained with the novel PermeaPad® barrier. The results showed that increased concentration of HP-β-CD leads to increased solubilization of the poorly soluble unionized ketoprofen, as well as hydrocortisone. However, this net increment of apparent solubility was not proportional to the increased flux measured. On the other hand, normalising the flux over the empirical free drug concentration, *i.e.*, the free fraction, gave a meaningful absolute permeability coefficient. The results achieved for the liposomal formulation were consistent with the finding on cyclodextrins. In conclusion, we proved the adequacy and usefulness of our method for calculating free drug fractions in the examined enabling formulations, supporting the validity of the established drug diffusion/permeation theory that the unbounded drug fraction is the main driver for drug permeation across a membrane.

1. Introduction

The effect of solubilization strategies on drug permeability and absorption is a debated topic, especially regarding colloidal solubilising agents. One example of such agents are cyclodextrins (CDs), a class of amphiphilic conical cyclic oligosaccharides with a hydrophilic outer surface and a hydrophobic core, which allows them to host hydrophobic moieties such as lipophilic portions of drug molecules (Fig. 1). Cyclodextrins offer an extraordinary solubility advantage, which over the years has led to their widespread use as a simple but effective enabling formulation (Fourmentin et al., 2020) with the added benefit of being excellent in taste masking (Astray et al., 2009; Walsh et al., 2014).

Although enhancement of apparent drug solubility is achievable with cyclodextrins, reports have emerged showing that the permeability and *in vivo* absorption are not significantly enhanced or are, in some cases, even reduced (Brewster et al., 2007; Dahan et al., 2010; Volkova et al., 2022). The complexation of drug, *D*, and cyclodextrin, *C*, often happens in a simple 1:1 ratio as described in Eq. (1).

$$D + C \rightleftharpoons DC \tag{1}$$

where *DC* is the complex formed. In ideal (*i.e.*, diluted) conditions, the equilibrium constant of complexation, $K_{1:1}$, is the parameter that characterises the stability of the complex and can be defined as:

* Corresponding author.
E-mail address: m.p.d.cagno@farmasi.uio.no (M.P. di Cagno).

https://doi.org/10.1016/j.ejps.2023.106559
Received 10 May 2023; Received in revised form 21 June 2023; Accepted 4 August 2023
Available online 5 August 2023

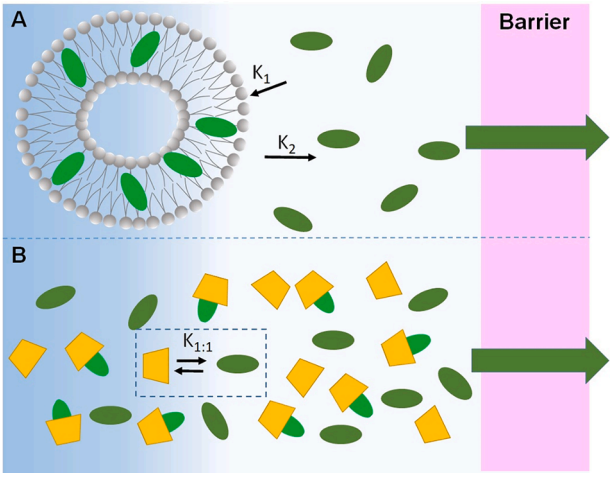

Fig. 1. Schematic representation of the solubility/permeability theory for: a) a liposomal dispersion and b) a cyclodextrin solution of a drug (green ovals). According to the solubility-permeability theory, the net flux of drug through the barrier (j) is mostly/solely determined by the free drug fraction (C_f, dark green ovals) rather than the complexed drug fraction (light green ovals).

$$K_{1:1} = \frac{C_{DC}}{C_D \times C_C} \quad (2)$$

where C_D and C_C are the free (or unbound) drug and cyclodextrin concentrations, respectively, and C_{DC} is the concentration of the complex.

Solubilization can also be achieved using nanosized vesicles such as liposomes comprising single or multiple concentric phospholipid bilayers dispersed in an aqueous environment (Fig. 1) (Douroumis and Fahr, 2013). In a liposomal dispersion loaded with a lipophilic compound, drug molecules are mainly distributed within the hydrocarbon tails of the phospholipids, with a limited amount also dissolved in the aqueous phase surrounding the vesicles, reaching a concentration close to or slightly higher than that of the drug's thermodynamic solubility (Di Cagno and Luppi 2013; Tzanova et al., 2022). Once the liposomal dispersion is created, the loaded (*i.e.*, liposomal) and unloaded (*i.e.*, free) drug fractions are at equilibrium, which is controlled by release (K_2) and loading (K_1) constants (Fig. 1). Enhancing drug solubility is only a step towards improving bioavailability, and the molecule's permeability often plays a crucial role in the *in vivo* outcome. The apparent permeability coefficient, P_{app} (cm/s), is the *in vitro* gold standard for evaluating/interpreting drug absorption. This parameter describes the drug transport rate, *i.e.*, the flux, j (μmol/cm^2 × s), through a biomimetic barrier normalised over the initial drug concentration in the donor, C_0 (mM) (Eq. (3)).

$$P_{app} = \frac{j}{C_0} \quad (3)$$

Miller and Dahan (2012) developed an interesting mathematical model based on a theoretical framework applied to the unstirred water layer theory to predict drug permeability of carbamazepine and hydrocortisone in the presence of cyclodextrins, demonstrating a good agreement with experimental *in vitro* data. For liposomal dispersions, it has been shown that even though liposomes increased drug solubility of lipophilic compounds, *e.g.*, hydrocortisone, the permeation of the drug through biomimetic barrier PermeaPad® (Wu et al., 2019) and *ex-vivo* tissues (Di Cagno and Luppi 2013) was not significantly increased. According to the most accepted theory on dissolution-permeation (Dahan et al., 2010; Miller et al., 2011; 2012), assuming one predominant ionization state of the drug, *i.e.*, a minimum two units' difference between pH and pKa, when solubilising agents such as cyclodextrins and liposomes are employed, the free drug concentration, C_f, should be considered as the real driving force for permeation and the absolute permeability, P_{abs}, calculated according to Eq. (4).

$$P_{abs} = \frac{j}{C_f} \quad (4)$$

Thus, from a theoretical perspective, by measuring the free drug fraction in the presence of cyclodextrins, it should be possible to predict drug permeability directly and, therefore, the *in vivo* performance of the formulation. The question arising is: Can empirical/mathematical predictions of free concentration be sufficient to interpret drug permeability of enabling formulations? Quite recently, Eriksen et al. (2023) demonstrated that, by utilising microdialysis in order to isolate the free drug fraction of colloidal dispersions, it was possible to obtain a good correlation with *in vitro* permeation data. On the other hand, Loftsson et al. (2002) demonstrated that cyclodextrins could unexpectedly induce real supersaturation, *i.e.*, an increase of the molecularly dissolved drug concentration above the thermodynamic solubility, through the formation of non-inclusion macromolecular complexes, which might unpredictably change the drug absorption rate. Recently, Butnarasu et al. (2022) reported that some acidic compounds, *e.g.*, ketoprofen, express a higher *in vitro* permeability than expected from the free drug fraction theory due to the formation of Ca^{2+}-coordinated dimers. This interesting finding might lead to the conclusion that the solubility/permeability theory based on free drug fraction (Dahan et al., 2010) might not always be able to interpret permeability when solubilizers are present (Fig. 1).

The aim of this work was to establish a correlation within the free drug fraction of different enabling formulations (cyclodextrin and liposomes) end drugs (atenolol, ketoprofen, hydrocortisone) at different ionization state pH2 and pH7.4). For doing that we systemically apply the analytical-computational method based on data fitting of diffusion profiles of drugs through unstirred water layers (Tzanova et al., 2022). For cyclodextrins, this unique method allows the precise and real-time simultaneous quantification of the equilibrium constant ($K_{1:1}$), diffusivity constants and concentrations of all three species involved: drug, cyclodextrin and drug-cyclodextrin complex. For liposomes, the method allows the quantification of the free drug fraction (C_D) and the drug loading (K_1) and release (K_2) constants. In the present study, we applied this method to obtain all aforementioned parameters for cyclodextrin dispersions of three model drugs (hydrocortisone, ketoprofen and atenolol) at different pH (7.4 and 2). Hydrocortisone and ketoprofen were chosen as they are well-known substrates for cyclodextrin complexation and because they are prone to supersaturation (Di Cagno and Luppi, 2013; Loftsson et al., 2002), whereas atenolol, a sparingly/very water-soluble compound at neutral/acidic pH, should not be a suitable substrate for cyclodextrins. We compared these data with *in vitro* permeability studies obtained employing the state-of-the-art PermeaPad® (Di Cagno et al., 2015) in multiwell-plate format (Jacobsen et al., 2019). In the current work, we also explored the role of free drug fraction in the permeation of hydrocortisone in the presence of liposomes.

2. Materials and methods

2.1. Materials and solvent solutions

Atenolol (≥ 98% TLC; ATN), hydrocortisone (≥ 98% HPLC; HC), ketoprofen (≥ 98% TLC, KTP) and sodium hydroxide (≥ 98.0% pellets; NaOH) were purchased from Sigma-Aldrich Chemie GmbH (Steinheim, DE), whilst potassium dihydrogen phosphate (KH_2PO_4), sodium dihydrogen phosphate dihydrate ($NaH_2PO_4{\cdot}2H_2O$), disodium phosphate dihydrate ($Na_2HPO_4{\cdot}2H_2O$) and sodium chloride (NaCl) were obtained from Merck KGaA (Darmstadt, DE). Pharmaceutical grade (2-hydroxypropyl)-β-cyclodextrin (M_w = 1501 g/mol; HP-β-CD) was purchased from CycloLab (Budapest, HU). All solutions were prepared with water, purified by a Milli-Q® water purification system for ultrapure water by Merck Millipore (Darmstadt, DE).

Phosphate-buffered saline (PBS, 73 mM) solutions with pH 7.4 and 2

were prepared as follows: for PBS pH 7.4, one part 2.5% (w/v) $NaH_2PO_4{\cdot}2H_2O$ solution was mixed with four parts 0.9% (w/v) $Na_2HPO_4{\cdot}2H_2O$ solution, whilst the PBS pH 2 was a 0.5% (w/v) KH_2PO_4 and 0.6% (w/v) $Na_2HPO_4{\cdot}2H_2O$ solution. The pH was adjusted to 7.4 ± 0.05 and 2 ± 0.05 (SevenCompact™ pH/ion metre S220; Mettler Toledo, Columbus, OH, USA) with NaOH pellets or 20% (v/v) H_3PO_4, respectively. The osmolality of both buffers was adjusted to 280−300 mOsm/kg (Semi-Micro Osmometer K-7400, Knauer, Berlin, DE) with NaCl, and the solutions were filtered 0.2 μm (Whatman® Nuclepore Track-Etch membrane filter; GE Healthcare Life Sciences, Maidstone, UK) before use.

2.2. Phase-solubility studies

CD solutions with the following concentrations were prepared: 0 (only PBS), 2.5, 10, 20, 30 and 50 mM. These were incubated with atenolol, ketoprofen or hydrocortisone solid powder for five days, thus creating saturated solutions with the respective API at growing CD concentrations. Each solution was filtered through a 0.2 μm PES syringe filter (VWR International, Radnor, PA, USA) and diluted adequately for the quantification using a UV/Vis microplate spectrophotometer at the wavelength of maximum absorbence, λ_{max}, given in Table 1. Each experiment was performed in duplicates. The equilibrium concentrations of each drug were plotted as a function of the CD concentration, and the binding constant, $K_{1:1}$ (M^{-1}), was determined from the *slope* of the diagram according to Higuchi and Connors' model (1965), as shown in Eq. (5). In this model, S_0 represents the thermodynamic solubility of the drug in the absence of CD.

$$K_{1:1} = \frac{slope}{S_0(1 - slope)} \tag{5}$$

2.3. Recording of drug diffusion profiles in unstirred water layer

The localised UV/Vis-spectroscopy method, earlier established by Di Cagno et al. (2018) and later developed by Di Cagno & Stein (2019), was applied to record drug diffusion profiles of the drug in water in the presence of CD, following the method previously described (Tzanova et al., 2021). Solutions of HP-β-CD (100 mM) and drug were prepared in PBS pH 7.4 and pH 2. Solutions of atenolol and ketoprofen at pH 7.4 had a concentration of 1 mM, while for ketoprofen at pH 2 and hydrocortisone, saturated solutions were prepared instead due to low solubility. Sample solutions were then prepared by mixing 1 mL of a drug solution with increasing amounts of the HP-β-CD solution and filling up to 2 mL with pure PBS, yielding a series of donor solutions with constant drug concentration (c_0) and increasing HP-β-CD concentrations (0, 2.5, 10, 25 and 50 mM). All samples were prepared 24 h prior to the analysis and stirred overnight at room temperature to ensure that complexation equilibrium was reached. The measurements were performed on a double-array UV/Vis spectrophotometer UV-6300 PC (VWR International, Radnor, PA, USA) in semi-micro cuvettes with PTFE stopper ($V_{chamber}$ = 700 μL, path length = 10 mm; Starna Scientific®, Essex, UK). Pure water (675 μL) was used as a diffusion medium and reference. At time zero, donor solution (25 μL) was injected at the bottom of the sample cuvette using a microneedle syringe (Hamilton Company, Reno, NV, USA). absorbence was recorded at 2-minute intervals at the specific maximum wavelength of absorbence (λ_{max}, Table 1) at precisely 0.51 cm from the bottom of the cuvette for 21 h. Drug diffusion profiles were then obtained by converting absorbence readings into concentration by the mean of drug-specific calibration curves ($R^2 \geq 0.999$).

2.4. Mathematical models and data fitting

Two different fitting procedures, *i.e.*, an analytical and a numerical approach, were employed to fit experimental data and to calculate diffusivities and equilibrium constants.

2.4.1. Analytical approach

The diffusion profiles obtained (Section 2.3) were fitted to the analytical solution of Fick's second law of diffusion presented by Di Cagno et al. (2018), Eq. (6):

$$c(x,\ t) = \frac{2A}{\sqrt{\pi}} \frac{e^{\frac{-x^2}{2\sigma^2+4Dt}}}{\sqrt{2\sigma^2 + 4Dt}} \tag{6}$$

where t is the time [*sec*] of the measurement and c is the concentration [mM] at that given time point, x is the distance between the origin of diffusion and detection point, whilst D [cm^2/s], A [$mmol/cm^2$] and σ [cm] are fitting parameters representing the drug diffusivity, initial drug fraction and the width of the initial drug distribution, respectively. The drug diffusivity coefficient in the presence of cyclodextrin and calculated by this model represents the average diffusivity, $\overline{D}$, of the free drug and the drug-cyclodextrin complex. Further fitting these values to Eq. (7) (Di Cagno and Stein, 2019) allows the estimation of the binding constant drug-cyclodextrin, $K_{1:1}$, and the diffusivities of the free drug, D_D, and complexed drug, D_{DC}.

$$\overline{D} = MF_{DC}D_{DC} + MF_DD_D = \frac{Q}{L_0}D_{DC} + \left(1 - \frac{Q}{L_0}\right)D_D$$
$$= D_D + \frac{Q}{L_0}(D_{DC} - D_D) \tag{7}$$

where MF_D and MF_{CD} are the molar fractions of free and bound drug, Q is the equilibrium concentration of the complex, and L_0 is the initial CD concentration.

2.4.2. Numerical approach

Drug diffusion profiles were fitted to the numerical model, as reported in our recent work (Tzanova et al., 2022), which allows the determination of the concentration of free and bound drug, in addition to the diffusivity of both species and the equilibrium binding constant, $K_{1:1}$. The model is based on a numerical solution of the diffusion equation, including a generative term, G_i (Eq. (8)).

$$\frac{\partial C_i(x,t)}{\partial t} = D_i\frac{\partial^2 C_i(x,t)}{\partial x^2} + G_i \tag{8}$$

where C_i and D_i represents the concentration and diffusion coefficient of the i^{th} diffusing species, respectively, t is the time and x is the diffusion path (assuming the diffusion to be significant only in one direction, *i.e.* the height of the cuvette). generative term G_i assumes different

Table 1
General characteristics of the investigated compounds (M_w, molecular weight; log*P*, partition coefficient octanol-water; *pKa*, acid dissociation constant; λ_{max}, wavelength of maximum absorbence; and ε, molar extinction coefficient) and concentrations of donor solutions for the diffusion experiments (c_0) (Section 2.3).

	M_w [g/mol]	log*P*[a]	pKa[a]	λ_{max} [nm]	ε [cm^2/mol]		c_0 [mM]	
					pH 7.4	pH 2	pH 7.4	pH 2
Atenolol (ATN)	266.34	0.16	9.58	225	9.52	9.10	0.501	0.501
Ketoprofen (KTP)	254.28	3.12	3.98	261	16.36	15.42	0.503	0.176
Hydrocortisone (HC)	362.46	1.61	–	248	15.85	15.57	0.329	0.375

[a] Source: PubChem.

expressions depending on the diffusing species – G_D, G_C and G_{DC} for the drug, cyclodextrin and drug-cyclodextrin complex, respectively. Hence, Eq. (8) can be solved for each species (as shown in Eqs. 9 – 11, where C denotes concentration, D – diffusion coefficient and M – molar weight; k_1 and k_2 are the kinetic constants for the complexation and dissociation of the drug-CD complex respectively, and m and n are the stoichiometric coefficients for the reaction).

$$\frac{\partial C_D}{\partial t} = D_D\frac{\partial^2 C_D}{\partial x^2} + G_D \; G_D = M_D\left(m * k_2 * C_{DC} - m * k_1 * \; C_D^m * C_C^n\right) \tag{9}$$

$$\frac{\partial C_C}{\partial t} = D_C\frac{\partial^2 C_C}{\partial x^2} + G_C \; G_C = M_C\left(n * k_2 * C_{DC} - n * k_1 * \; C_D^m * C_C^n\right) \tag{10}$$

$$\frac{\partial C_{DC}}{\partial t} = D_{DC}\frac{\partial^2 C_{DC}}{\partial x^2} + G_{DC} \; G_{DC} = M_{DC}\left(k_1 * \; C_D^m * C_C^n - k_2 * C_{DC}\right) \tag{11}$$

Boundary conditions for the series of equations imply impermeable walls at both ends of the cuvette, whilst the initial conditions consider that no drug is present in the cuvette except the one residing within the injected solution volume. Further, assuming uniform initial concentrations of all species in the injected donor solution, the attainment of the thermodynamic equilibrium can be evaluated by solving Eqs. (12)–14.

$$C_{DCE} = \frac{k_1}{k_2} * \; C_{DE}^m * C_{CE}^n \tag{12}$$

$$\left(C_{DE} + C_{DCE} m \frac{M_D}{M_{DC}}\right) V_s = C_{D0} V_s \tag{13}$$

$$\left(C_{CE} + C_{DCE} n \frac{M_C}{M_{DC}}\right) V_s = C_{C0} V_s \tag{14}$$

where V_s represents the injected volume, C_{D0} and C_{C0} are the drug and cyclodextrin concentrations used to prepare the injected solution, and C_{DE}, C_{CE}, and C_{DCE} are the drug, cyclodextrin and complex equilibrium concentrations (*i.e.* the initial concentration values in the injected volume), respectively. Eq. (12) describes the attainment of equilibrium between the drug, cyclodextrin and complex concentrations and Eqs. (13) and 14 express the mass balance referring to the drug and cyclodextrin in the injected volume. The iterative numerical solution (implicit Euler method, tolerance 10^{-8}) of these equations allows the determination of the concentration of the individual species at equilibrium. A more detailed description of the mathematical approaches is presented in our original work (Tzanova et al., 2022).

2.5. Permeability experiments with PermeaPad® plate

Permeability of atenolol, ketoprofen and hydrocortisone through an artificial biomimetic barrier at pH 7.4 and 2 both in the absence and presence of increasing amounts of HP-β-CD (2.5, 10, 20, 30 and 50 mM) was investigated using the high-throughput 96-well PermeaPad® plate (InnoMe GmbH, Espelkamp, DE). In the same system, the permeability of hydrocortisone from liposomal dispersions tested earlier in diffusion studies (Tzanova et al., 2022) was analysed both undiluted and diluted 1:2 and 1:4. PBS pH 7.4 was used as acceptor solution (400 μL) in all cases. The donor (200 μL) consisted of a saturated API solution in either pure PBS or a HP-β-CD solution (same solutions used in the phase-solubility study, section 2.2; C_0) or the liposomal dispersion. The plate was incubated in an orbital shaker-incubator (ES-20, Biosan, Riga, LV) at 25 °C and agitated at 200 rpm for 5 h. Samples (100 μL) were withdrawn from the acceptor compartment every 30 min and replaced with fresh PBS. Drug concentrations in the samples were determined by spectrophotometric measurements on a Spectramax 190 Microplate Reader (Molecular Devices Inc., Sunnyvale, CA, USA) at drug-specific wavelengths shown in Table 1. Standard solutions (calibration curve $R^2 \geq 0.999$) were measured on the same plate, and blank absorbence (PBS) was deducted from all measurements. Experiments were repeated in at least a triplicate ($n = 3 – 6$). Flux values (j) were calculated from the slopes of the linear parts of the permeation curves (Q/A *vs* t, where Q is the cumulative amount of drug permeated, A is the membrane area 0.13 cm^2, and t is time). These values were further normalised by total starting concentration (C_0) or by free drug concentration (C_D) in order to obtain the apparent (P_{app}) and the absolute (P_{abs}) permeability as outlined in Eqs. (3) and (4), respectively.

3. Results and discussion

In this work, we investigated the diffusivity and permeability of three model drugs, both as simple saturated drug solutions and oversaturated solutions with HP-β-CD. Additionally, the permeability of hydrocortisone from a liposomal dispersion, characterised in our previous study (Tzanova et al., 2022), was also investigated.

3.1. Cyclodextrins

Equilibrium constants of drug-cyclodextrin at pH 7.4 and 2, were evaluated through three different approaches: a classical phase-solubility study and the analytical and numerical data fitting of drug diffusivity profiles. The results are reported in Tables 2 and 3. For hydrocortisone and ketoprofen at both investigated pH values, the classical phase-solubility approach introduced by Higuchi & Connors (1965) revealed a type A_L behaviour, *i.e.*, a steady linear increase of apparent drug solubility with increased HP-β-CD concentration (Table 2). This observation is in accordance with the available literature reports (*e.g.*, Messner et al., 2011; Sridevi and Diwan, 2002). Atenolol, on the other hand, demonstrated a relatively high aqueous solubility at both pHs (73 mM at pH 7.4 and 264 mM at pH 2), owing to its positive charge in both investigated environments, which leads to the inefficient solubilization effect provided by HP-β-CD. The presence of charge on a drug molecule makes its incorporation into the cyclodextrin molecule's hydrophobic cavity difficult and the complex's stability is quite low. Thus, it was impossible to estimate a reliable $K_{1:1}$ due to the nature of the Higuchi & Connors' approach (Eq. (5)), which depends on the linear regression of the increased apparent drug solubility as a function of cyclodextrin concentration, as this increase was not observed.

An alternative approach to calculate this parameter is to study drug diffusion through the unstirred water layer (UWL) by localised spectroscopy (Di Cagno and Stein, 2019). The results from the analytical and numerical solutions of the diffusion equation (described in Sections 2.4.1 and 2.4.2, respectively) seem to be in good agreement with each other, with some variations in absolute numbers (Table 3). Unlike the phase-solubility approach, both data-fitting methods provided a binding constant value for atenolol. Independently of the pH and the mathematical approach used, the values of the binding constant atenolol-(HP-β-CD) were extremely low, varying from 9 to 26 M^{-1}. These results confirm the particularly low binding tendency between atenolol and HP-β-CD observed in the phase-solubility studies. A significant

Table 2
Apparent solubility of atenolol (ATN), ketoprofen (KTP) and hydrocortisone (HC) measured at increasing HP-β-CD concentrations in the phase-solubility study (Section 2.2). The same solutions (C_0) were used in the PermeaPad® plate permeability experiments (Section 2.5).

HP-β-CD [mM]	C_0 [mM]					
	pH 7.4			pH 2		
	ATN	KTP	HC	ATN	KTP	HC
0	73.44	35.10	0.94	264.34	0.38	0.75
2.5	70.74	37.91	2.31	217.44	1.18	2.25
10	75.65	36.26	6.27	207.66	4.08	5.90
20	71.10	41.10	12.53	221.52	8.12	12.01
30	88.76	48.95	16.86	289.76	12.01	16.88
50	105.22	57.67	28.86	300.58	19.90	26.82

Table 3
Binding constants ($K_{1:1}$) of atenolol (ATN), ketoprofen (KTP) and hydrocortisone (HC) to HP-β-CD at pH 7.4 and 2, calculated from phase-solubility study (Section 2.2) and the analytical and numerical approaches (Section 2.4). Values presented as: calculated value ± CI limit (analytical); and average ± SD for $n = 4$ (different CD concentrations; numerical). No SD provided for the phase-solubility results because $n = 2$.

	$K_{1:1}$ [M^{-1}]					
	pH 7.4			pH 2		
	Phase-solub.	Analytical	Numerical	Phase-solub.	Analytical	Numerical
ATN	NA*	19 ± 6**	9 ± 0	NA*	26 ± 14**	9 ± 0
KTP	19	252 ± 41	272 ± 0.1	2361	573 ± 151	272 ± 0
HC	1438	729 ± 85	791 ± 25	1262	986 ± 112	806 ± 0

* NA, not applicable. The determination of $K_{1:1}$ using phase-solubility diagrams was not possible for ATN.
** Based on a two-parameter fitting, assuming no complex is present, *i.e.* diffusivity of the bound drug (D_b) is equal to zero.

Table 4
Flux values (j) calculated from the PermeaPad® plate permeability experiments (Section 2.5) with saturated drug solutions at pH 7.4 and 2 and with various concentrations of HP-β-CD. Values presented as average ± standard deviation (SD) for $n = 3$–6.

HP-β-CD [mM]	j ± SD [× 10^{-5} μmol/cm^2·s]					
	pH 7.4			pH 2		
	ATN	KTP	HC	ATN	KTP	HC
0	39.6 ± 0.3	33.3 ± 3.3	0.631 ± 0.048	50.7 ± 1.6	0.286 ± 0.047	0.465 ± 0.030
2.5	32.2 ± 1.1	26.1 ± 0.6	0.579 ± 0.008	46.3 ± 1.0	0.728 ± 0.106	0.438 ± 0.070
10	34.3 ± 1.3	21.9 ± 1.6	0.775 ± 0.039	47.8 ± 1.1	1.479 ± 0.146	0.713 ± 0.034
20	33.2 ± 2.4	21.9 ± 0.6	0.890 ± 0.047	48.3 ± 1.5	1.957 ± 0.274	0.626 ± 0.071
30	27.5 ± 0.0	15.5 ± 0.8	0.679 ± 0.132	46.5 ± 2.4	2.099 ± 0.639	0.672 ± 0.077
50	34.4 ± 2.5	10.7 ± 1.5	0.891 ± 0.227	47.5 ± 4.9	2.460 ± 0.271	0.666 ± 0.120

advantage of the numerical approach is that following only a single experimental injection, it is possible to extract information about all species involved in the complexation, *i.e.*, the drug, the cyclodextrin and the drug-cyclodextrin complex. Moreover, this method yielded more accurate and precise results in terms of data output, with a much lower standard deviation than the other two methods. For ketoprofen and hydrocortisone, the two mathematical approaches generated practically identical values for the binding constants at pH 7.4 (Table 3). They are in reasonably good agreement with each other and the phase-solubility results for hydrocortisone at pH 2. On the other hand, for ketoprofen at pH 2, the analytical and numerical results are lower than the phase-solubility studies (four and eight times, respectively). Generally, drugs containing carboxylic acid groups show a higher binding constant in their unionised form, *i.e.*, at acidic pH (Di Cagno, 2016). This is indeed what the phase-solubility data suggests for ketoprofen. However, the drug diffusion results would indicate no significant difference in binding constant between the two different pHs for this drug. As the mathematical fitting is performed on experimental data of drug diffusion in UWL, it is, as such, absolute. It is, therefore, possible to hypothesise that the phase-solubility approach for ketoprofen might be prone to error regarding the binding constant. One possible explanation of the discrepancy between diffusion and phase-solubility results for ketoprofen is that the stoichiometry of the complex ketoprofen-(HP-β-CD) might not be 1:1 at pH 2. Drug-cyclodextrin complexes tend to self-assemble in aqueous solutions to form aggregates at high cyclodextrin concentrations (Saokham et al., 2018). Loftsson et al. (2002) demonstrated that drug-cyclodextrin complexes can self-associate to form larger water-soluble aggregates, which further solubilized ketoprofen through non-inclusion complexation. This phenomenon would be quantified in a phase-solubility study as active complexation.

The results from the permeability experiments performed with the PermeaPad® plate are summarised in Table 4. These data show that in the absence of cyclodextrin (0 mM conc.), atenolol exhibited the largest flux of the three drugs in both pH environments examined due to its superior solubility compared to ketoprofen and hydrocortisone (Table 2) and despite its charged state. Ketoprofen is predominantly charged at pH 7.4, making the compound sparingly soluble at this pH (35.3 mM, Table 2), thus creating a large enough concentration gradient between the donor and acceptor and a consequent high flux in the absence of cyclodextrin. At acidic conditions, the amount of ketoprofen dissolved at thermodynamic equilibrium was much lower than that measured at neutral pH, thus generating a much lower flux. No significant differences in solubility and flux were observed for hydrocortisone in the different pH environments. This findings are logical as hydrocortisone does not contain ionizable groups and therefore its thermodynamic solubility is practically unaffected by pH changes.

The relative changes in flux in the presence and absence of HP-β-CD were calculated to ease the comparison of the results (Fig. 2). For atenolol, adding cyclodextrin had a marginal effect on the total amount of drug dissolved, as mentioned previously, and had an overall negative impact on the flux. This effect was more pronounced at pH 7.4, where higher number of atenolol molecules are neutral and available for complexation, thus being prevented from permeating than at pH 2. No further correlation was observed between the increased concentration of cyclodextrin and the decreased flux. For hydrocortisone, the effect of adding HP-β-CD to the solution was overall positive for all concentrations of the complexing agent. However, no further correlation was observed also in this case. Unlike atenolol, hydrocortisone complexation with HP-β-CD significantly positively affected the apparent solubility, which could explain the measured increase in flux. Ketoprofen exhibited a pH-dependent behaviour, representing the most interesting case in this study. At neutral pH, increased amounts of HP-β-CD reduced the net drug flux, whereas the exact opposite was observed at acidic pH. At pH 2, where the flux of ketoprofen through the biomimetic barrier increased significantly at the higher concentrations of cyclodextrin.

According to Fick's law, the flux of a drug through a barrier is concentration-dependent. This implies that flux of drug solutions with different donor concentrations, C_0 (Table 2), cannot be compared directly. A better parameter in terms of comparability is the apparent permeability coefficient, P_{app}, which is classically calculated by dividing the flux by the drug concentration in the donor compartment, C_0, (Eq. (3)). Our P_{app} results, summarised in Fig. 3, show no significant change in atenolol's apparent permeability in the presence of HP-β-CD, as the coefficient value remains relatively constant at lower HP-β-CD concentrations ($\leq$ 20 mM) and only drops slightly at the higher concentrations investigated. Significant differences between the pH values can also be seen for atenolol at every cyclodextrin concentration. These differences are reasonable as the drug showed lower overall permeability at acidic pH, *i.e.*, where all molecules are expected to be protonated and charged (Amirdehi et al., 2017). On the other hand, Fig. 3 displays a pattern of reduction in apparent permeability for both hydrocortisone and ketoprofen with increasing HP-β-CD concentrations. Further, it should be noted that the initial decrease in apparent permeability upon introducing the complexing agent is twice as pronounced for hydrocortisone as for ketoprofen.

These results are contradictory as, from a theoretical perspective, P_{app} solely reflects the interaction within the drug molecule and the biomimetic barrier to cross and therefore it should be, to some extent, a constant. The permeability results reported in Fig. 3 show this approximation to be correct for atenolol, but for ketoprofen and hydrocortisone

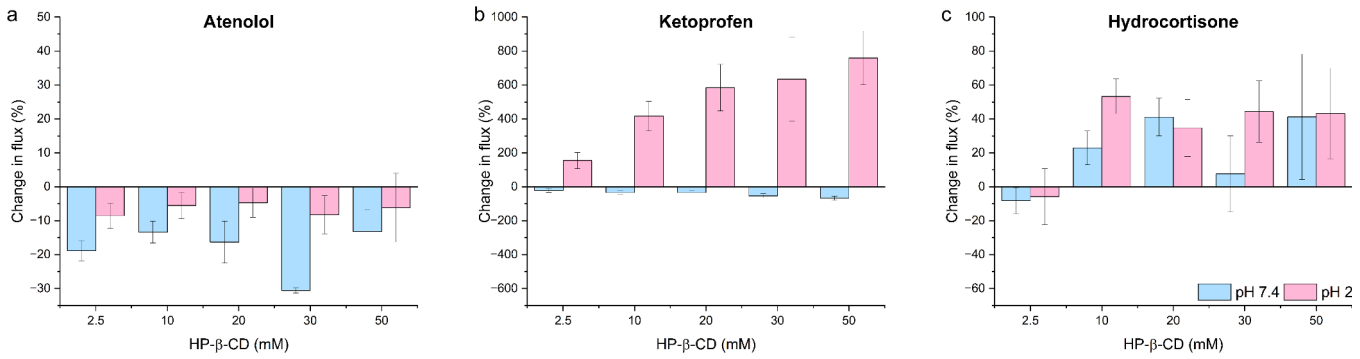

Fig. 2. Relative changes in atenolol (a), ketoprofen (b) and hydrocortisone (c) flux through biomimetic PermeaPad® barrier in the presence of increasing concentration of HP-β-CD at pH 7.4 (blue) and pH 2 (pink).

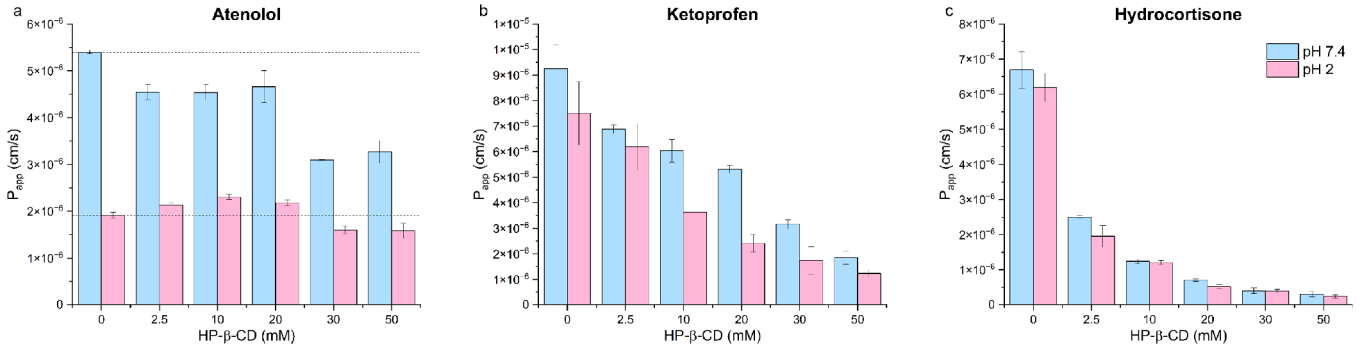

Fig. 3. Apparent permeability coefficients, P_{app}, (Eq. (3)) of atenolol (a), ketoprofen (b) and hydrocortisone (c) through biomimetic PermeaPad® barrier in the absence and presence of increasing concentration of HP-β-CD at pH 7.4 (blue) and pH 2 (pink). Horizontal lines show the level of P_{app} in the absence of the cyclodextrin, aiding the comparison to the other cases.

(*i.e.*, the compounds that show moderate/high affinity for HP-β-CD), the apparent permeability significantly decreases and is not indicative of the actual drug accumulation in the acceptor compartment. Hence, normalising the flux over the total drug concentration, C_0, is clearly an inadequate way to interpret permeability/absorption in such cases. A more appropriate interpretation of drug permeability in the presence of solubilizers and enabling formulations is offered by the dissolution/permeation theory introduced by Miller et al. (2011; 2012). In this case, permeability is interpreted by the normalisation of the flux by the free drug concentration, C_D (Eq. (4)).

To explore this idea further, we studied drug diffusion in the absence of HP-β-CD and the presence of increasing amounts of the complexing agent with the localized UV-spectroscopy approach (Tzanova et al., 2022). This method, coupled with mathematical modelling (Section 2.4.2) allows the extraction of diffusion coefficients of all species as well as free drug ($C_f = C_D$ in the case of cyclodextrins), free cyclodextrin (C_C) and drug-cyclodextrin complex (C_D) concentrations (Tzanova et al., 2022). A complete summary of all data-fitting parameters is presented in

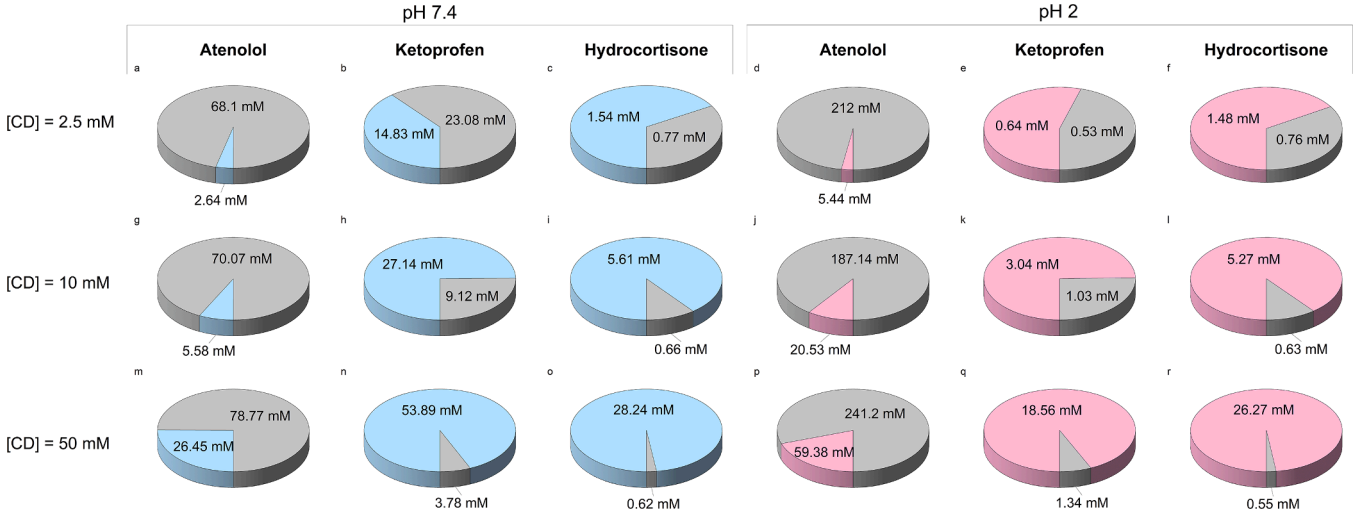

Fig. 4. Percentage of the total drug concentration, which can be attributed to the free (grey part; C_D) and bound to cyclodextrin (coloured part; C_{DC}) drug for atenolol, ketoprofen and hydrocortisone at pH 7.4 (pies with blue) and pH 2 (pies with pink) in the presence of increasing concentration of HP-β-CD. Numbers show absolute concentration values, calculated from the ratio [$C_{DE}/C_{D0,no\ CD}$] in diluted conditions (after solving Eqs. (12)-14).

the Appendix (Table A1), whilst Fig. 4 shows the composition of each solution in terms of where the drug can be found – *free, i.e.*, molecularly dissolved (in grey colour) or bounded, *i.e.*, complexed (in blue or pink colour according to the pH), to HP-β-CD along with the exact concentrations for each species. The figure clearly illustrates the minor influence of the cyclodextrin on the net solubility of atenolol at both investigated pH values (*i.e.*, grey part dominant) with only a marginal increase in bound-drug fraction up to a total of 25% and 20% at pH 7.4 and pH 2, respectively. The complete opposite is evident for hydrocortisone, which is almost completely (~ 98%) incorporated inside the cyclodextrin cavities at the highest investigated HP-β-CD concentration. In fact, already upon dissolving hydrocortisone in as little at 2.5 mM HP-β-CD solution, over half (~ 66–67%) of the apparently dissolved drug seems to exist in a complex with the cyclodextrin. Negligible differences between the investigated pH environments can also be reported for hydrocortisone. Contrary, ketoprofen presents an interesting case of pH-dependence of solution composition. At pH 7.4 and at the lowest cyclodextrin concentration, most of the drug remains molecularly dissolved, with only about 38% being complexed, whereas 55% is bound to HP-β-CD at acidic pH. The fractions even out for the two pHs at the higher concentrations of complexing agent, and the bound-drug fraction increases significantly (up to 93%), albeit not as completely as the case is with hydrocortisone. Although the free drug fraction of ketoprofen decreases at pH 2, the free drug concentration increases from 0.38 mM in the absence of cyclodextrin to 0.53 mM at 2.5 mM HP-β-CD and further up to 1.34 mM at 50 mM HP-β-CD (Table 2 and Fig. 4). On the other hand, when the ketoprofen-(HP-β-CD) complex is exposed to a more neutral environment, the free drug concentration significantly decreases from 23 mM (2.5 mM HP-β-CD) to 3.8 mM (50 mM HP-β-CD). This is precisely the observation made in the permeability studies, where a net increase of the ketoprofen flux with increased cyclodextrin concentration is measured only at pH 2, whilst the flux decreases at pH 7.4. Thus, the permeation behaviour is in agreement with the calculated change in free drug concentrations at both pHs.

Regarding the absolute permeability coefficient, P_{abs} (Eq. (4)), the permeability values for all investigated compounds are more similar across the entire range of HP-β-CD concentrations (Fig. 5). In fact, for atenolol, P_{abs} is nearly constant for each pH, as indicated by the horizontal dashed lines in Fig. 5. The superior permeability at pH 7.4 is again confirmed, following the theory (Henderson-Hasselbalch equation), which suggests that at pH 2 atenolol is orders of magnitude more charged than at pH 7.4, thus having a lower permeability. For ketoprofen and hydrocortisone, P_{abs} generally appears to increase slightly at both pHs at increased concentrations of cyclodextrin. The absolute permeability of hydrocortisone remains unaffected at the lower concentrations and increases slightly only to reach a plateau around 10 mM (or lower) HP-β-CD. However, this increasing trend persists throughout the investigated cyclodextrin concentration range for ketoprofen. The increase is more pronounced at pH 7.4, which can be correlated to the decreasing concentration of free drug mentioned previously. The increase in P_{abs} at pH 2 is directly proportional to the increasing free drug concentration (Fig. 4 and Appendix Table A2**)** under these conditions.

It is necessary to underline that the diffusion studies from which the free drug fraction (Fig. 4) was estimated were performed in unsaturated (*i.e.*, diluted) solutions, whereas the permeability studies were performed at saturated conditions and this might explanation slight variation of the P_{abs} (*e.g.*, the slight discrepancy for atenolol). The significant enhancement in measured flux for hydrocortisone at higher concentration of CD might be linked to supersaturation of hydrocortisone (Di Cagno and Luppi, 2013) which can't be detected in diluted conditions, *i.e.*, where the C_f has been determined. Another plausible explanation, is the formation of macromolecular drug complex at interface which own higher permeability through the barrier. This phenomenon has been observed for ketoprofen *in vitro* permeation tests where mucus was involved (Butnarasu et al., 2022). In any cases, the mathematical projections of the free drug fraction seem to support the conceptual dissolution/permeation framework, *i.e.*, the free drug fraction is the main driving force pushing *in vitro* drug absorption rather than the total drug concentration (Dahan et al., 2010).

3.2. Liposomes

A simple hydrocortisone-loaded liposomal formulation was prepared, and the drug diffusion was studied in our earlier work (Tzanova et al., 2022). In the current project, we have expanded this formulation's investigation to include hydrocortisone's permeability through biomimetic PermeaPad® barrier in the case of undiluted and diluted suspension. Fig. 6 summarises the results for flux and the two different permeability coefficients, P_{app} and P_{abs}.

The flux of hydrocortisone across the membrane is gradually reduced due to formulation dilution, which is intuitively logical since the total drug available for permeation is diminished. However, this reduction does not correspond to the decrease in total drug concentration, as a 1:4 dilution only halves the flux. In fact, when the flux values are normalised over the total drug concentration, the apparent permeability coefficient seems to increase (solid green columns in Fig. 6). For comparison, these values are still 4–10 times smaller than the P_{app} of the drug solution ($6.11 \pm 0.64 \times 10^{-6}$ cm/s).

The flux values for the liposomal samples correlate very well with the concentration of free drug ($R^2 = 0.954$), both of which decrease with increasing dilution factor. Consequently, calculating the absolute permeability coefficient for each case yields almost identical values, as expected. Interestingly, these values are even more constant than the P_{abs} for any of the drug-cyclodextrin complex situations studied. This can be explained by the slower kinetics of exchange between free and encapsulated drug in the case of liposomes. Additionally, the liposomal system offers significantly lower flexibility in terms of drug-drug interactions, reducing the number of potential, influential exchanges within the system, which might alter the permeability of the drug.

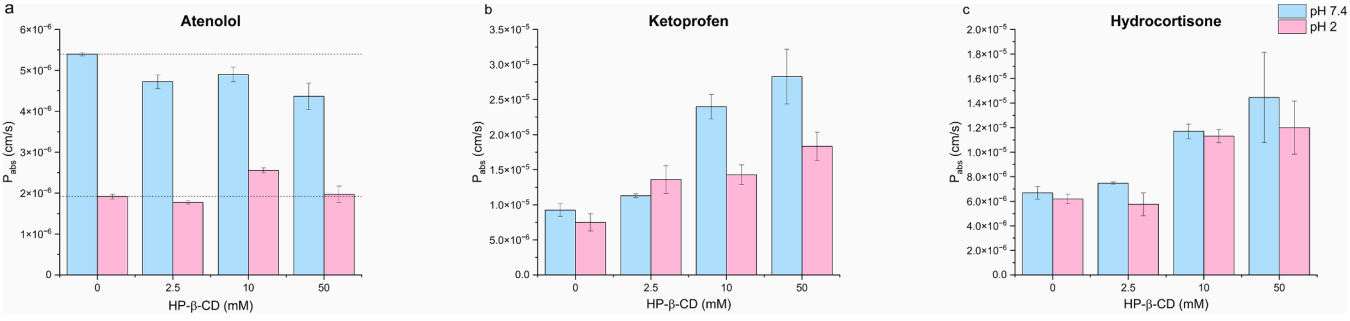

Fig. 5. Absolute permeability coefficients, P_{abs}, (Eq. (4)) at pH 7.4 (blue columns) and pH 2 (pink columns) for atenolol (a), ketoprofen (b) and hydrocortisone (c) through biomimetic PermeaPad® in the absence and presence of increasing concentration of HP-β-CD. Horizontal lines show the level of P_{app} in the absence of the cyclodextrin, aiding the comparison to the other cases.

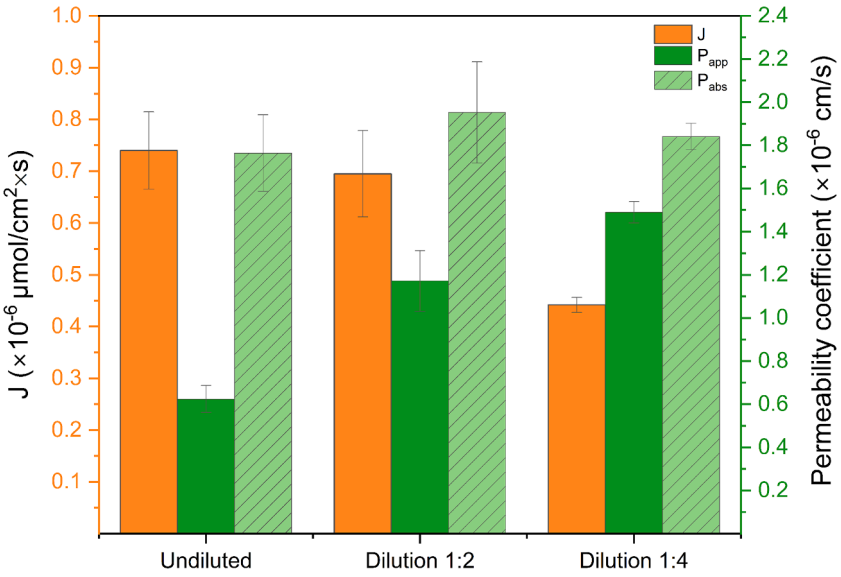

Fig. 6. Flux (*j*; orange) and permeability coefficients (apparent, P_{app}, and absolute, P_{abs}, in solid and striped green, respectively) of hydrocortisone through biomimetic PermeaPad® from liposomal dispersions at different concentrations at pH 7.4.

4. Conclusions

In this work, we demonstrated that solubilising drugs with cyclodextrins may or may not enhance drug permeation properties and that the outcome is chemical-space dependent. In the case of drug solubilization using liposomal systems, drug permeability can be directly correlated to the concentration of free drug available for permeation. We proved that for cyclodextrins, mathematical fitting of drug diffusivity in UWLs allows not only the quantification of diffusivities and free drug fraction but also provides a much more accurate method for determining binding constants in comparison to other available methods, such as phase-solubility studies. Our findings clearly demonstrate the validity of the drug dissolution/permeation theory introduced by Miller et al. (Dahan et al., 2010; Miller et al., 2011, 2012), pointing at the free drug concentration as the main driver in drug absorption when enabling formulations are employed. However, we noticed that an interpretation of permeability based only on mathematical prediction might lead to imprecise estimation in some specific and limited cases. Given the sustainable transition pharmaceutics is facing, the authors recommend combining *in silico* with *in vitro* studies to obtain the best *in vivo* predictions without the need for animal testing.

CRediT authorship contribution statement

Martina M. Tzanova: Conceptualization, Methodology, Formal analysis, Investigation, Data curation, Writing – original draft, Writing – review & editing, Visualization. **Lisa Nguyen:** Methodology, Validation, Formal analysis, Investigation, Data curation, Writing – review & editing. **Federica Moretti:** Software, Methodology, Formal analysis, Investigation, Data curation, Writing – review & editing. **Mario Grassi:** Software, Methodology, Formal analysis, Writing – review & editing. **Greta Camilla Magnano:** Investigation, Writing – review & editing. **Dario Voinovich:** Writing – review & editing. **Paul C. Stein:** Methodology, Software, Writing – review & editing. **Marianne Hiorth:** Resources, Writing – review & editing, Supervision. **Massimiliano Pio di Cagno:** Conceptualization, Methodology, Resources, Data curation, Writing – original draft, Supervision, Project administration.

Declaration of Competing Interest

Massimiliano Pio di Cagno, the corresponding and leading author of this article, is Scientific Consultant for Phabioc GmbH, the producer of the PermeaPad®.

Data availability

Data will be made available on request.

Acknowledgements

The authors are grateful to Phabioc GmbH for providing the PermeaPad® products used in this work. The authors would also like to express their gratitude to Bente Amalie Breiby, Ivar Grove and Tove Larsen from University of Oslo for the technical support and to the NordicPop consortium (NordForsk project No. 85352) which has contributed the development of this research.

Supplementary materials

Supplementary material associated with this article can be found, in the online version, at doi:10.1016/j.ejps.2023.106559.

References

Amirdehi, M.A., Pousti, M., Asayesh, F., Gharib, F., Greener, J., 2017. Solvent effects on acid–base equilibria of propranolol and atenolol in aqueous solutions of methanol: UV-spectrophotometric titration and theory. J. Solut. Chem. 46 (3), 720–733. https://doi.org/10.1007/s10953-017-0595-x.

Astray, G., Gonzalez-Barreiro, C., Mejuto, J.C., Rial-Otero, R., Simal-Gándara, J., 2009. A review on the use of cyclodextrins in foods. Food Hydrocoll. 23 (7), 1631–1640. https://doi.org/10.1016/j.foodhyd.2009.01.001.

Brewster, M.E., Noppe, M., Peeters, J., Loftsson, T., 2007. Effect of the unstirred water layer on permeability enhancement by hydrophilic cyclodextrins. Int. J. Pharm. 342 (1), 250–253. https://doi.org/10.1016/j.ijpharm.2007.04.029.

Butnarasu, C., Caron, G., Pacheco, D.P., Petrini, P., Visentin, S., 2022. Cystic fibrosis mucus model to design more efficient drug therapies. Mol. Pharmaceut. 19 (2), 520–531. https://doi.org/10.1021/acs.molpharmaceut.1c00644.

Dahan, A., Miller, J.M., Hoffman, A., Amidon, G.E., Amidon, G.L., 2010. The solubility–permeability interplay in using cyclodextrins as pharmaceutical solubilizers: mechanistic modeling and application to progesterone. J. Pharm. Sci. 99 (6), 2739–2749. https://doi.org/10.1002/jps.22033.

Eriksen, J.B., Christiansen, J.J., Bauer-Brandl, A., Ruponen, M., Rautio, J., Brandl, M., 2023. In-vitro dynamic dissolution/bioconversion/permeation of fosamprenavir using a novel tool with an artificial biomimetic permeation barrier and microdialysis-sampling. Eur. J. Pharm. Sci. 181, 106366 https://doi.org/10.1016/j.ejps.2022.106366.

Di Cagno, M.P., 2016. The potential of cyclodextrins as novel active pharmaceutical ingredients: a short overview. Molecules 22 (1), 1. https://doi.org/10.3390/molecules22010001.

Di Cagno, M.P., Bibi, H.A., Bauer-Brandl, A., 2015. New biomimetic barrier Permeapad™ for efficient investigation of passive permeability of drugs. Eur. J. Pharm. Sci. 73, 29–34. https://doi.org/10.1016/j.ejps.2015.03.019.

Di Cagno, M.P., Clarelli, F., Våbenø, J., Lesley, C., Rahman, S.D., Cauzzo, J., Stein, P.C., 2018. Experimental determination of drug diffusion coefficients in unstirred aqueous environments by temporally resolved concentration measurements. Mol. Pharm. 15 (4), 1488. https://doi.org/10.1021/acs.molpharmaceut.7b01053.

Di Cagno, M.P., Luppi, B., 2013. Drug "supersaturation" states induced by polymeric micelles and liposomes: a mechanistic investigation into permeability enhancements. Eur. J. Pharm. Sci. 48 (4–5), 775–780. https://doi.org/10.1016/j.ejps.2013.01.006.

Di Cagno, M.P., Stein, P.C., 2019. Studying the effect of solubilizing agents on drug diffusion through the unstirred water layer (UWL) by localized spectroscopy. Eur. J. Pharm. Biopharm. 139, 205–212. https://doi.org/10.1016/j.ejpb.2019.04.005.

Douroumis, D., Fahr, A., 2013. Liposomes As Intravenous Solubilizers For Poorly Water-Soluble Drugs. United Kingdom: John Wiley & Sons, Incorporated, United Kingdom, pp. 37–66.

Fourmentin, S., Crini, G.g., & Lichtfouse, E. (2020). The history of cyclodextrins(1st ed. 2020. ed., Vol. 52).

Higuchi, T., Connors, K.A., 1965. Phase-solubility techniques. Adv. Anal. Chem. Instrum. 4, 117–210.

Jacobsen, A.-C., Krupa, A., Brandl, M., Bauer-Brandl, A., 2019. High-throughput dissolution/permeation screening—a 96-well two-compartment microplate approach. Pharmaceutics 11 (5), 227. https://doi.org/10.3390/pharmaceutics11050227.

Loftsson, T., Magnúsdóttir, A., Másson, M., Sigurjónsdóttir, J.F., 2002. Self-association and cyclodextrin solubilization of drugs. J. Pharm. Sci. 91 (11), 2307–2316. https://doi.org/10.1002/jps.10226.

Messner, M., Kurkov, S.V., Palazón, M.M., Fernández, B.Á., Brewster, M.E., Loftsson, T., 2011. Self-assembly of cyclodextrin complexes: effect of temperature, agitation and media composition on aggregation. Int. J. Pharm. 419 (1), 322–328. https://doi.org/10.1016/j.ijpharm.2011.07.041.

Miller, J.M., Beig, A., Carr, R.A., Webster, G.K., Dahan, A., 2012. The solubility–permeability interplay when using cosolvents for solubilization: revising the way we use solubility-enabling formulations. Mol. Pharmaceut. 9 (3), 581–590. https://doi.org/10.1021/mp200460u.

Miller, J.M., Beig, A., Krieg, B.J., Carr, R.A., Borchardt, T.B., Amidon, G.E., Dahan, A., 2011. The solubility–permeability interplay: mechanistic modeling and predictive application of the impact of micellar solubilization on intestinal permeation. Mol. Pharmaceut. 8 (5), 1848–1856. https://doi.org/10.1021/mp200181v.

Miller, J.M., Dahan, A., 2012. Predicting the solubility–permeability interplay when using cyclodextrins in solubility-enabling formulations: model validation. Int. J. Pharm. 430 (1–2), 388–391. https://doi.org/10.1016/j.ijpharm.2012.03.017.

Saokham, P., Muankaew, C., Jansook, P., Loftsson, T., 2018. Solubility of cyclodextrins and drug/cyclodextrin complexes. Molecules 23 (5), 1161. https://doi.org/10.3390/molecules23051161.

Sridevi, S., Diwan, P.V.R., 2002. sOptimised transdermal delivery of ketoprofen using pH and hydroxypropyl-β-cyclodextrin as co-enhancers. Eur. J. Pharm. Biopharm. 54 (2), 151–154. https://doi.org/10.1016/S0939-6411(02)00056-5.

Tzanova, M.M., Moretti, F., Grassi, G., Stein, P.C., Hiorth, M., Abrami, M., di Cagno, M. P., 2022. Modelling drug diffusion through unstirred water layers allows real-time quantification of free/loaded drug fractions and release kinetics from colloidal-based formulations. Eur. J. Pharm. Biopharm. 178, 168. https://doi.org/10.1016/j.ejpb.2022.08.009.

Tzanova, M.M., Randelov, E., Stein, P.C., Hiorth, M., Di Cagno, M.P., 2021. Towards a better mechanistic comprehension of drug permeation and absorption: introducing the diffusion-partitioning interplay. Int. J. Pharm. 608, 9. https://doi.org/10.1016/j.ijpharm.2021.121116.

Volkova, T.V., Simonova, O.R., Perlovich, G.L., 2022. Permeability of diverse drugs through a lipid barrier: impact of pH and cyclodextrin. J. Mol. Liq. 357, 119135 https://doi.org/10.1016/j.molliq.2022.119135.

Walsh, J., Cram, A., Woertz, K., Breitkreutz, J., Winzenburg, G., Turner, R., Tuleu, C., 2014. Playing hide and seek with poorly tasting paediatric medicines: do not forget the excipients. Adv. Drug. Deliv. Rev. 73, 14–33. https://doi.org/10.1016/j.addr.2014.02.012.

Wu, I.Y., Bali, S., Skalko-Basnet, N., Di Cagno, M.P., 2019. Interpreting non-linear drug diffusion data: Korsmeyer-Peppas model to study drug release from liposomes. Eur. J. Pharm. Sci. 138, 105026 https://doi.org/10.1016/j.ejps.2019.105026.